UV-Laser-Induced Decomposition of Kapton Studied by Infrared Spectroscopy

E. E. Ortelli,[†,‡] F. Geiger,[†] T. Lippert,[*,†] J. Wei,[†,‡] and A. Wokaun[†,‡]

General Energy Research, Paul Scherrer Institut, 5232 Villigen PSI, Switzerland, and Departement of Chemical Engineering and Industrial Chemistry, Swiss Federal Institute of Technology, ETH Zentrum, 8092 Zürich, Switzerland

Received March 3, 2000; Revised Manuscript Received April 25, 2000

ABSTRACT: The UV-laser (308 nm)-induced decomposition and ablation of polyimide (Kapton) was studied using diffuse reflectance infrared Fourier transform (DRIFT) spectroscopy. The samples were prepared with a special technique (SiC substrates) allowing analysis of surface species of the laser-treated polymer. The first step of photolysis is the simultaneous decomposition of the imide ring, between the nitrogen and carbonyl carbon atom, and of the diaryl ether group. The functional groups belonging to the corresponding amide and carbonyl system are detected. In the next step the aromatic system decomposes, and isocyanates, aliphatic hydrocarbons, nitriles, and alkynes are formed. Volatile species compatible with this decomposition mechanism (CO, CO_2, HCN, and C_2H_2) are detected by additional mass spectrometry measurements.

Introduction

During the past three decades, since the commercialization of Kapton polyimide, an impressive variety of polyimides have been synthesized.[1,2] Polyimides possess outstanding key properties, such as thermooxidative stability,[3] high mechanical strength,[4] high modules, excellent electrical[5] and optical properties,[6,7] and superior chemical resistance.[8] Recently, polyimides have also been applied as membranes for gas separation.[9,10] Approximately 15 years ago the direct structuring or laser ablation of polyimides by excimer lasers was described first.[11,12] These studies showed clearly that ablation caused clean etching of the material with micron size precision. Because of the importance of polyimides in numerous applications and the difficulty in etching these polymers by other means, such findings prompted intensive further research.[13] At the present time laser ablation of polyimide is a routine part in microelectronic packaging[14,15] and the fabrication of nozzles for ink jet printer heads.[16] In addition, laser irradiation is being explored as means of generating uniform thin polymer films, which may also prove to be useful in electronic packaging as well as in other applications such as polyimide film coating of various materials.[17] As discussed above, the term *polyimides* refers to a group of polymers. Most ablation studies, including this, have been conducted on one specific polyimide, known as Kapton. Kapton is produced commercially by DuPont, using a condensation reaction of pyromellitic dianhydride (PMDA) and oxydianiline (ODA), with polyamic acid as intermediate, as shown in Figure 3. During laser ablation the incident radiation is absorbed within some finite volume of the material, unless the material is completely transparent at the laser wavelength. Kapton shows a broad UV absorption band in the UV region between 180 and 400 nm, allowing the effective absorption of all common excimer laser wavelengths (193, 248, 308, and 351 nm).[18] It is generally agreed on that the mechanism is mainly photothermal, with additional photochemical features, especially at 193 nm irradiation.[19] Prominent features of Kapton ablation are the sharp ablation threshold (measured with atomic force microscopy, AFM), Arrhenius tails (smooth Arrhenius-type ablation onset, measured with mass spectrometry or quartz microbalance, QMB), and differences in the ablation rate near the threshold between two very sensitive methods, i.e., AFM and QMB.[20] The lower threshold fluences are obtained by QMB, suggesting the additional or exclusive ejection of gaseous molecules at low fluences (maybe even below the"threshold" of ablation). Ablation products have been studied by a variety of techniques. Infrared spectroscopy,[21] gas chromatography,[22] and mass spectrometry[23] have been used to identify the principal gaseous products of Kapton ablation: CO_2, CO, H_2O, HCN, and various light hydrocarbons (up to four carbon atoms). Laser-induced fluorescence measurements indicate that diatomic fragments C_2 and CN are also formed at least transiently during ablation.[24] Larger molecules (e.g., C_{60}) up to visible carbon particles are also formed.[25] The soot is partly redeposited around the ablation crater and consists of amorphous carbon with some crystalline features. The ablated area of Kapton was also analyzed, and carbonization in a certain fluence range was detected.[26] This carbonization results in an increase of the conductivity of up to 12 orders of magnitude.[27] The carbonized material consists of amorphous carbon, but also graphitic material.[28] Other surface species, intermediates, and products in the polymer film which could be indicative of a mechanistic scheme are not reported to our knowledge. The analysis of the surface of polymers is quite difficult. The laser radiation is absorbed within a layer of 100 nm (at 308 nm) of the polymer film, thus resulting in changes within a very thin layer.

The analytical method of choice should be sensitive enough to analyze the surface and should also be capable of identifying changes of specific groups in the polymer chains. One promising candidate is infrared (IR) spectroscopy, which is an important method for the

[†] Paul Scherrer Institut.
[‡] Swiss Federal Institute of Technology.
* Corresponding author. Fax ++41-(0)56-310-2199; e-mail thomas.lippert@psi.ch.

10.1021/ma000389a CCC: $19.00
Published on Web 06/13/2000

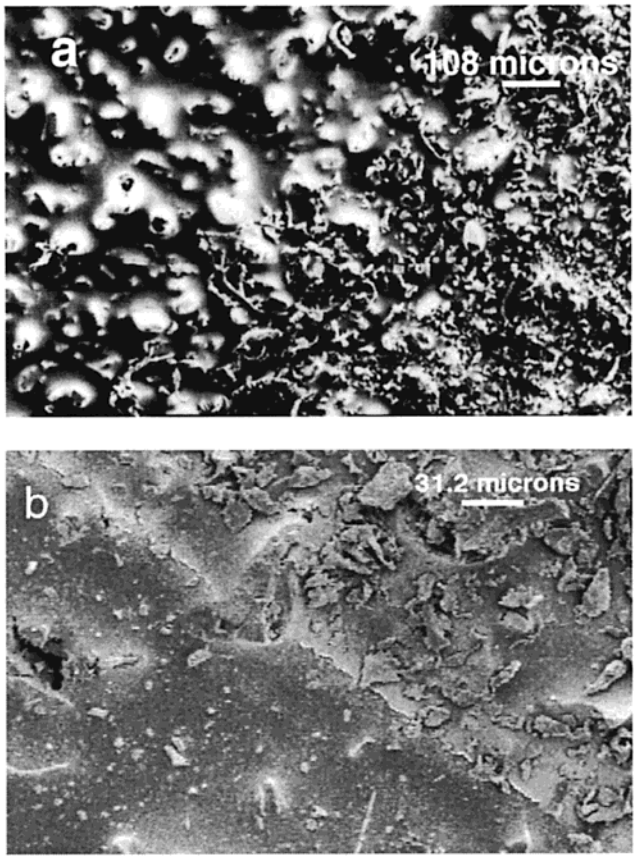

Figure 1. Scanning electron microscopy (SEM) pictures of a SiC disk. (a) In the lower right part of the picture the abraded Kapton is visible as scrapes. (b) The border between laser-treated and untreated area is shown. The lower left side corresponds to the laser treated area (20 pulses at 155 mJ cm^{-2}).

characterization of polymer conformation,[29] orientation,[30] and solvent effects.[31] Newer developments in IR spectroscopy include time-resolved[32,33] and two-dimensional techniques[34,35] for dynamic processes in polymers, such as conformational changes, diffusion, and polymerization. The standard technique for IR spectroscopy is transmission spectroscopy, which is not suitable for our purpose, because the polymer films are too thick and the method is not sensitive enough for surface species. A surface sensitive technique such as attenuated total reflection (ATR)[36] or diffuse reflectance infrared Fourier transform (DRIFT) spectroscopy should be suitable for the investigation of the polymer films after laser irradiation. ATR spectroscopy is suited for the analysis of samples with flat surfaces, e.g. polymer films, but it is well-known that surface structures and roughening of the polymer films take place during ablation. In one study ATR was used to examine polymer films after irradiation in a relatively small fluence range.[37] Diffuse reflectance infrared Fourier transform (DRIFT) spectroscopy is specifically designed to study powdered sample and is well-known for its high sensitivity. A wide variety of materials can be analyzed using DRIFT spectroscopy. Some of these materials can be analyzed in substance, without any sample preparation. In previous works diffuse reflectance spectra of polymer films were collected by placing KBr powder over the sample.[38] Unfortunately, the quality, the amount, the size of the used particle, and how they are packed in the sample holder significantly affect the scattering characteristics of the overlayer material and therefore the quality of the spectra.[39] This problem can be overcome by the use of a silicon carbide (SiC) sampling kit.

The XeCl-laser (308 nm)-induced decomposition of Kapton is studied to identify reaction steps leading to the previously mentioned gaseous products and to identify the intermediate steps of the surface carbonization of Kapton. The XeCl laser is applied in the industrial processing of polyimide due to the reliability of optical and laser components at the emission wavelength (308 nm). The Kapton samples are studied after irradiation at various laser fluence and laser repetition rates.

Experimental Section

Kapton HN (DuPont) foils with a thickness of 125 μm were obtained from Goodfellow. For the irradiation a XeCl excimer laser (Lambda Physik Compex 205) emitting at 308 nm was used. The mass spectra were obtained with a V.G. Monitorr 100D quadrupole mass spectrometer (QMS) operated in a vacuum. The sample was positioned in front of the electron impact ionizer of the QMS at a distance of 1 cm. For the experiments the QMS was operated in the scan-analog mode using the Faraday cup. The mass resolution is 0.1 amu. The emission spectra were measured with Acton SpectraPro monochromator equipped with a Princeton Instruments CCD camera. The DRIFT measurements were performed using a Bruker EQUINOX 55/S FTIR equipped with a liquid nitrogen cooled mercury−cadmium−telluride (MCT) detector. All the samples were analyzed in a diffuse reflectance unit (Specac). The SiC disks (Spectra-Tech[40]) are used to abrade the surface of Kapton, resulting in a coverage of the SiC disk by polymer scrapes, as shown in Figure 1a. The SiC disk is mounted on a holder which can be used for the laser irradiation and the DRIFT cell. Spectra were obtained from the accumulation of at least 1024 scans at a resolution of 4 cm^{-1}. The size of the IR beam on the sample is smaller than 0.6 mm^2, ensuring that only the irradiated part (typically ~25 mm^2) of the SiC disk is measured in the DRIFT unit.

DRIFT spectra are usually presented in Kubelka−Munk units. In this work we prefer to present the spectra as relative reflectance units (I/I_0). The reflectance of the abraded polymer changes upon irradiation. The SiC substrate is grayish-black and absorbs strongly throughout the whole mid-IR region. These properties violate one of the basic assumptions of the Kubelka−Munk theory, i.e., the presence of a nonabsorbing or weakly absorbing substrate;[41] therefore, reflectance units are used. The spectra shown in the figures (with the exception of the reference spectrum of polyimide in Figure 2) are difference spectra between the material before and after laser treatment. An increase of surface species corresponds to an increase of the absorption and therefore to negative peaks (going down) and peak areas. The peaks that are going up denote a decreasing band, due to the reduced absorption of disappearing species. For the analysis of the laser-induced decomposition mechanism of Kapton several relevant vibrational frequencies are chosen which are important for the decomposition mechanism. A detailed assignment of all bands can be found in the literature.[42−47] The assignment of the polyimide bands is mainly based on model compounds, see e.g. the thorough study by Ishida et al.,[43] which could also be used for many products identified in this study.

Results

Reference Spectra and Assignment of Bands. The reference spectrum (Figure 2) of Kapton obtained with the SiC sampling method agrees well with previous published data. Several bands in the reference spectrum (Figure 2) and also in the corresponding scheme of the synthesis of Kapton (Figure 3) are marked with letters (A−G). These bands are used in the discussion about the decomposition mechanism.

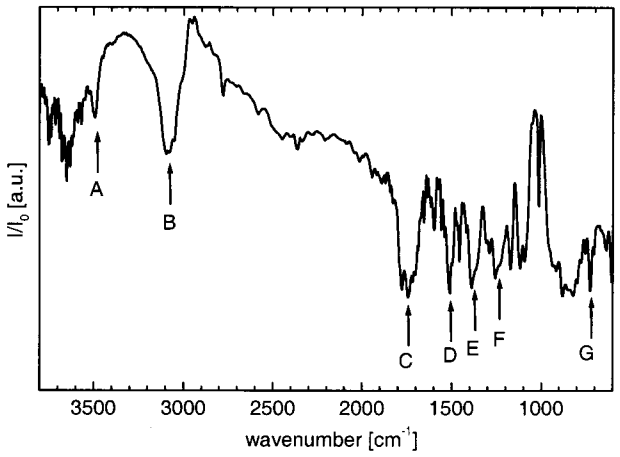

Figure 2. DRIFT spectrum of Kapton; 1024 scans with a resolution of 4 cm^{-1} and using SiC as background. The following bands are assigned: (A) 3490 cm^{-1}: N−H stretching; (B) 3060 cm^{-1}: C−H stretching; (C) 1740 cm^{-1}: C═O stretching; (D) 1500 cm^{-1}: aromatic ring stretching; (E) 1390 cm^{-1}: C−N stretching; (F) 1260 cm^{-1}: C_{ar}−O−C_{ar} stretching of aryl ether; (G) 725 cm^{-1}: out-of-plane bending of the imide ring.

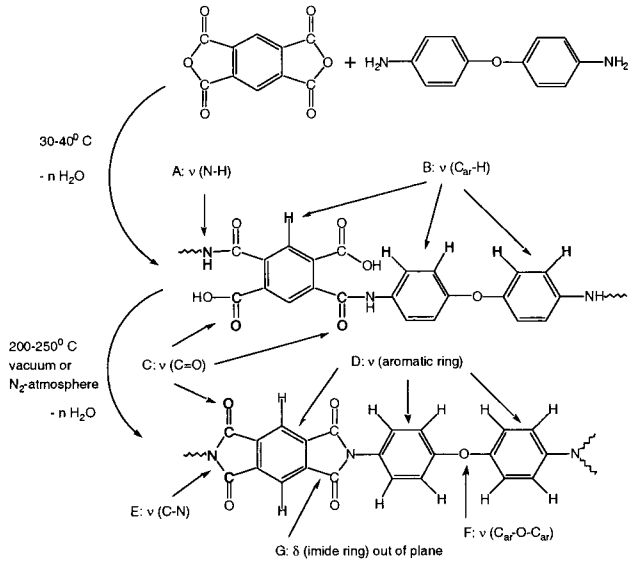

Figure 3. Scheme of the synthesis of Kapton. Some bands relevant for the discussion are marked (bold) and assigned.

In the high wavenumber regions two bands are prominent: a sharp band at 3490 cm^{-1} (denoted A in Figure 2) and a broad absorption at 3080 cm^{-1} (denoted B). The first band is assigned to the N−H stretching vibration of polymer chain end groups and NH groups of polyamic acid, due to an incomplete imidization during the synthesis. Band B belongs to the C−H stretching vibrations of the aromatic rings. The broad band around 1740 cm^{-1} (denoted C) is due the C═O stretching vibration of the imide ring. The sharp peaks at 1600 and 1500 cm^{-1} (band D) are assigned to the stretching vibrations of the aromatic systems, i.e., the 1,2,4,5-tetrasubstituted and the 1,4-disubstituted ring. The broad absorption at 1390 cm^{-1} (band E) is assigned to the C−N stretching in the imide ring while the band at 1260 cm^{-1} (band F) is assigned to the asymmetric C_{ar}−O−C_{ar} stretching vibration of the diaryl ether group. The sharp band at 725 cm^{-1} (band G) corresponds to the out-of-plane bending vibration of the imide ring.

Laser Ablation of Kapton with 308 nm Irradiation. The laser ablation of Kapton at 308 nm has been studied previously in detail.[28] An ablation threshold of 40 mJ cm^{-2} has been determined for the same Kapton samples and the same experimental setup as in this study. The term ablation threshold is defined in this study as the laser fluence necessary to remove polymer material in the irradiated area, measured by a profilometer. For this study we used laser fluences below, at, and above the threshold of ablation of Kapton films.

Irradiation of the SiC Substrate. The stability of the SiC disks under laser ablation conditions was tested first. A spectrum of a SiC disk was used as background. The difference spectra of the SiC disk after irradiation with the highest fluence applied in this study (155 mJ cm^{-2}) was measured after various pulse numbers (50, 100, 500, and 5000) and at the highest repetition rate (10 Hz). No changes in the spectra were observed, suggesting that SiC is stable under the applied conditions.

Kapton Irradiated with 80 mJ cm^{-2}. For the first experiments a fluence (80 mJ cm^{-2}) well above the threshold fluence of ablation (40 mJ cm^{-2}) was applied. To test the general feasibility of our approach, a variation of the general procedure was used. The sample used for the reference spectrum was irradiated with 50, 150, 500, and 500 pulses at a repetition rate of 10 Hz. After each irradiation a DRIFT spectrum was measured. As expected, all bands are decreasing in intensity, indicating a continuous decomposition of the polymer. This shows that it is possible to follow the decomposition of polyimide using difference spectra up to several thousand of pulses, with no artifacts, e.g., carbonization, interfering with the measurements.

In the following experiments the SiC disk with abraded Kapton was used as background spectrum. The disk was irradiated with various pulse numbers, and spectra were taken after each irradiation.

Irradiation at the Threshold of Ablation: 40 mJ cm^{-2}. To identify possible intermediates of the laser-induced decomposition of Kapton, the threshold fluence of ablation was chosen. At this fluence ablation is just starting, and changes in the material should be slow, giving the best chance to monitor intermediates.

The freshly prepared sample was irradiated with various pulse numbers (500, 1500, 3500, 7500, 15 500, and 31 500) at a repetition rate of 10 Hz. After each irradiation the DRIFT spectra was measured. The spectra are shown in Figure 4. After 500 pulses several bands are growing in intensity, i.e., 1730, 1500, 1375, 1245, 830, and 725 cm^{-1}, whereas only two bands are decreasing, i.e., 1390 and 1260 cm^{-1}. We also observe an absorption increase over the whole mid-IR region, denoted by the rising baseline. This increase of the baseline has already been reported previously and was assigned to an accumulation of carbonaceous species in and surrounding the irradiated area.[38,46] With increasing pulse numbers only few bands are increasing further (1730, 1500, 1375, and 1245 cm^{-1}), but additionally bands are decreasing now (1780, 1745, 1515, 1390, 1260, 830, and 725 cm^{-1}). To analyze the changes in the DRIFT spectra in more detail, a semiquantitative analysis was performed. The peak areas of several bands are plotted versus the pulse numbers, as shown in Figures 5 and 6.

The two bands at 1780 and 1745 cm^{-1} reveal a very similar behavior. Both are decreasing in a very similar fashion (as shown for the 1780 cm^{-1} band in Figure 5,

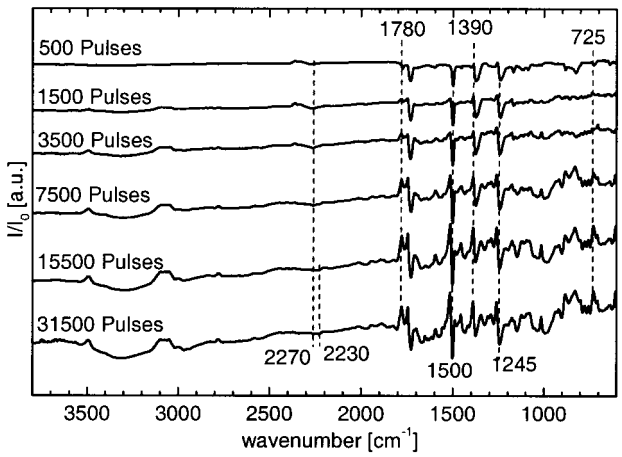

Figure 4. DRIFT difference spectra of Kapton obtained with an accumulation of 1024 scans. The untreated SiC supported Kapton was used as background. The sample was irradiated at 10 Hz with 40 mJ cm^{-2} with various pulse numbers. The relevant bands are marked with their exact location.

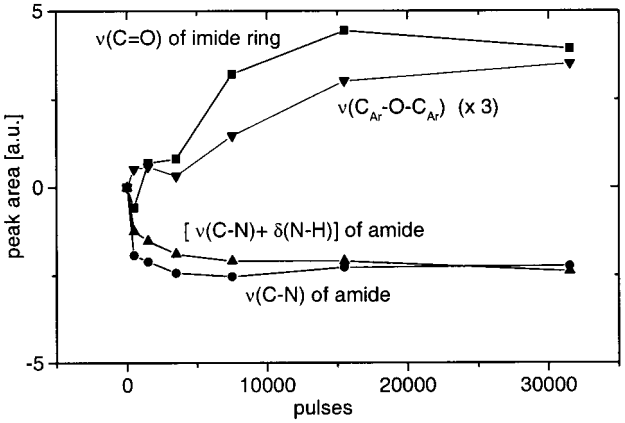

Figure 5. Changes of the peak areas as a function of the pulse number for the following bands: at 1780 cm^{-1} the C═O stretching vibration of the imide ring (■); at 1375 cm^{-1} the C−N stretching vibration of the amide (●); at 1500 cm^{-1} the combination band: C−N stretching vibration and N−H deformation of the amide (▲); and at 1260 cm^{-1} the C_{ar}−O−C_{ar} stretching vibration (▼).

■ as symbol). Therefore, we assign them to the doublet of the C═O stretching vibration of the imide ring, whereas the increasing band at 1730 cm^{-1} is assigned to a carbonyl functional group of an open ring species. This could be the amide structure (called also amide I band) and/or the aryl−C═O structure (both are shown in Figure 7). The changes of the peak areas of the C−N stretching vibration of the imide ring at 1390 cm^{-1} and of the out-of-plane bending of the imide ring at 725 cm^{-1} are very similar to the one shown for the imide carbonyl peak (shown in Figure 5).

The increasing bands at 1730, 1500, 1375, and 1245 cm^{-1} follow very similar trends. The band at 1500 cm^{-1} is assigned to the combination band of the N−H deformation and the C−N stretching vibration (also named amide II band, shown as ▲ in Figure 5). The band at 1375 cm^{-1} is assigned to the C−N stretching band of an amide (also named amide III band, shown as ● in Figure 5), while the band at 1245 cm^{-1} is assigned to the C_{ar}−O stretching vibration (see Figure 7) from the decomposed diaryl ether group.

Amide bands are not present in cyclic imides but are typical for the intermediate of the Kapton synthesis, the

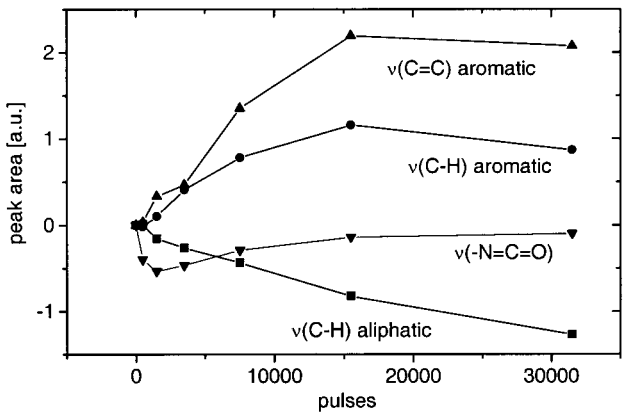

Figure 6. Changes of the peak areas as a function of the pulse number for the following bands: at 2950 cm^{-1} the C−H stretching vibration of aliphatic hydrocarbons (■); at 3080 cm^{-1} the C−H stretching vibration of aromatic hydrocarbons (●); at 1515 cm^{-1} the aromatic ring stretching vibration (▲); at 2270 cm^{-1} the −N═C═O stretching vibration (▼).

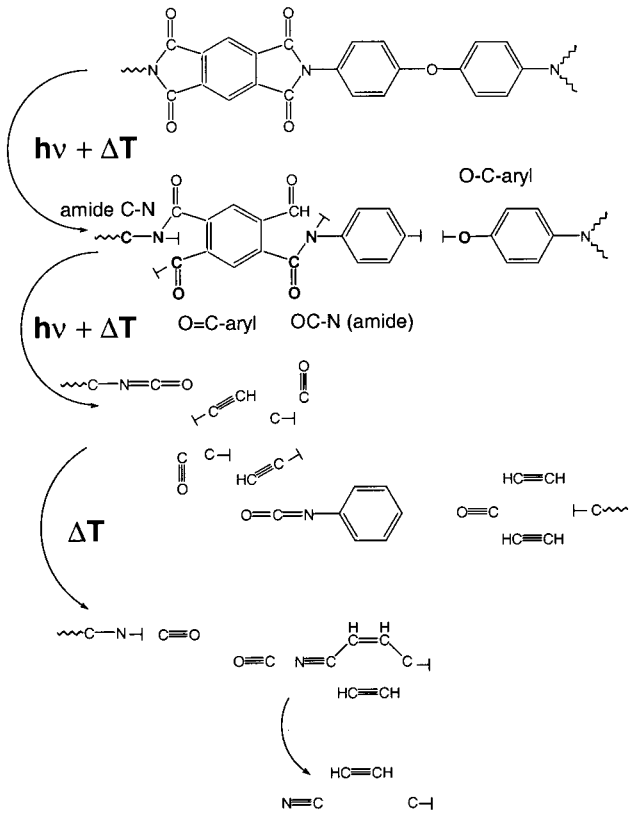

Figure 7. Suggested decomposition scheme. Several bands are marked (bold) and assigned. ⊥ indicates a broken bond; information on the character (radicalic, ionic, terminated) is not available from the present experiments.

polyamic acid. All of the above-mentioned increasing bands reveal changes of the peak areas very similar to the two representations shown in Figure 5. The decomposition of the imide system is characterized by the decrease of the carbonyl bands, of the C−N stretching vibration, and of the out-of-plane bending vibration of the imide system.

Upon further irradiation other increasing bands are detected. A broad absorption around 3320 cm^{-1} with a shoulder at higher wavenumbers is developed. This is assigned to the C−H stretching vibration of acetylenes and to the N−H stretching vibration of amides, which are typically between 3200 and 3400 cm^{-1}. All of these

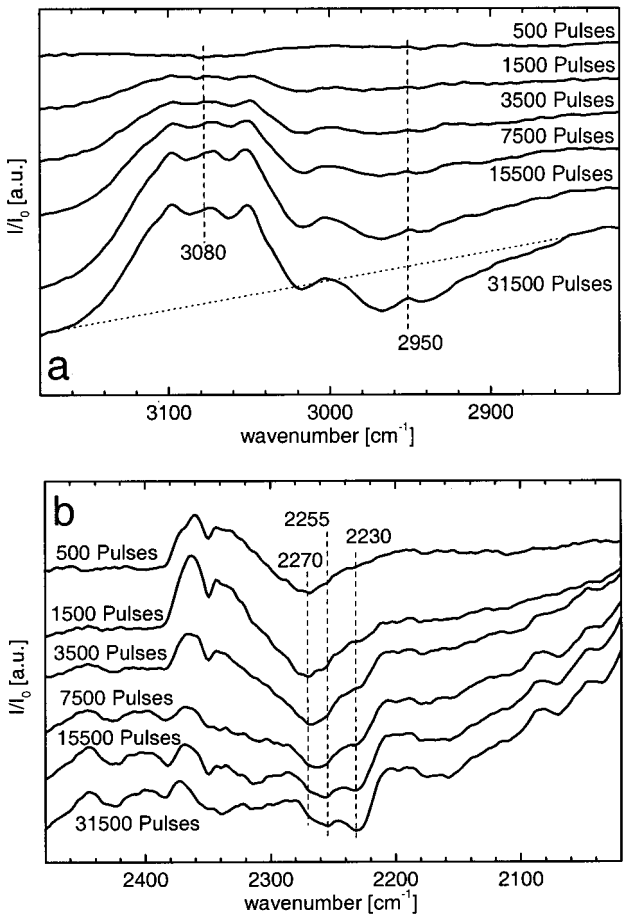

Figure 8. Magnification of two regions in the DRIFT spectra of Kapton presented in Figure 4. (a) Region of C−H stretching vibrations: at 3080 cm^{-1} aromatic hydrocarbons; at 2950 cm^{-1} aliphatic hydrocarbons. The baseline applied for the peak area calculation is shown as dotted line in the spectrum for 31 500 pulses. (b) Region of conjugated double bonds and triple bonds: at 2270 cm^{-1} the −N═C═O stretching vibration; at 2255 cm^{-1} the −C≡C− stretching vibration; and at 2230 cm^{-1} the −C≡N stretching vibration. Around 2350 cm^{-1} the typical doublet of gas-phase CO_2 is present.

bands show, as discussed above, a similar behavior and reveal more or less the exact mirror image of the previously described decreasing bands.

Three bands distinguish the aromatic system: the broad C−H stretching band around 3080 cm^{-1} (a magnification is shown in Figure 8a, and ● in Figure 6) and the ring stretching vibrations at 1600 and 1515 cm^{-1} (▲ in Figure 6). All of these bands decrease upon laser irradiation, as shown in Figure 6, revealing the decomposition of the aromatic systems. Another significant band in the IR spectra of Kapton is the C_{ar}−O−C_{ar} stretching vibration at 1260 cm^{-1} of the aromatic ether. The decrease of the peak area suggests that this group is also one of the primary decomposition sites.

Growing bands are detected around 2950 cm^{-1} and can be assigned to C−H stretching vibrations of aliphatic groups (magnification shown in Figure 8). There are no aliphatic C−H groups present in Kapton; therefore, we can assign these groups to reaction products. The increase of the peak area is different from the previous described changes. The peak area increases nearly linear with laser pulses, as shown in Figure 6 (■ as symbol). Further identification of the aliphatic chains is very difficult because of the complex band structure in the region where for example C−C (1260−700 cm^{-1}), C═C (1680−1620 cm^{-1}), C−O (1270−1060 cm^{-1}), and C−N bonds (1420−1400 cm^{-1}) are absorbing. A very interesting region in the mid-IR spectra is between 2300 and 2100 cm^{-1}. There are only few groups absorbing in this region. Most of these groups are characterized by strong and sharp absorption. In Figure 8b magnification of this region is shown. The broad absorption around 2350 cm^{-1} is the typical doublet of gas-phase CO_2. Carbon dioxide is a very IR-active molecule, and slight changes in the concentration, e.g., due to variations in the compressed air purge or slightly different purge times, will cause continuous changes in the intensity of the CO_2 band. Around 2270 cm^{-1} a growing band can be observed. With increasing pulse numbers the band starts to decrease (shown with ▼ as symbol in Figure 6), while new bands at 2255 and 2230 cm^{-1} are getting more pronounced with increasing pulse numbers. The peak at 2270 cm^{-1} can be assigned to the asymmetric −N═C═O stretching vibration of an isocyanate species and the two bands at the lower wavenumbers to the stretching vibration of alkynes (−C≡C−) and nitrile (−C≡N) groups.

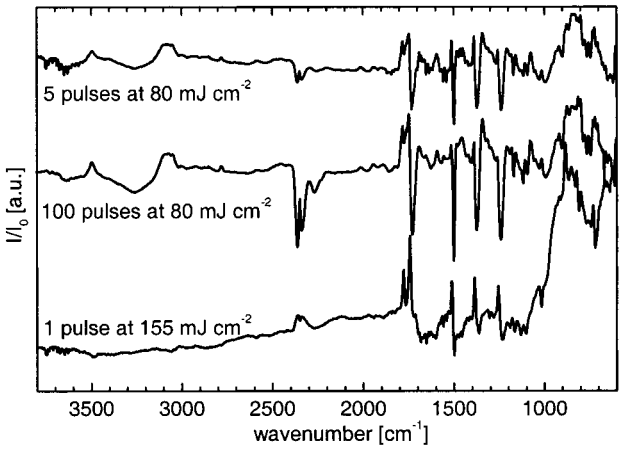

Figure 9. DRIFT difference spectra of Kapton irradiated with fluences above the threshold of ablation (80 and 155 mJ cm^{-2}) are shown.

Irradiation above the Threshold of Ablation: The applied fluences were increased to a level well above the threshold of ablation to test whether the previously described changes in the DRIFT spectra are really due to ablation.

80 mJ cm^{-2}. The freshly prepared sample was irradiated with 1, 2, 5, 10, 20, 50, and 100 pulses at a repetition rate of 10 Hz. In Figure 9 the spectra recorded after 5 and 100 pulses are shown. After the first pulse several bands are growing in intensity (going down: at 1730, 1500, 1370, and 1245 cm^{-1}) while others are decreasing (1780, 1745, 1600, 1515, 1390, 830, and 725 cm^{-1}). All bands assigned to the imide ring are decreasing (1780, 1745, 1390, and 725 cm^{-1}) whereas the bands assigned to the amide and aryl−carbonyls groups are increasing. After 100 pulses the bands assigned to the isocyanate and nitrile group (2270 and 2230 cm^{-1}) are clearly present. The bands at lower wavenumbers (<1100 cm^{-1}) are more difficult to observe, due to the steeply increasing background. This is most probably due to accumulation of carbon species in the irradiated area.[38,46] The changes in the spectra are very similar to the data described previously for irradiation with 40 mJ cm^{-2}. Only 100 pulses are needed to reach a similar state of decomposition as compared to the 31 500 pulses at 40 mJ cm^{-2}. This shows clearly that for the present

flux we are observing the ablative decomposition of Kapton, for which a sharp threshold of ablation is observed.

To study the influence of the laser repetition rate on the decomposition of Kapton, a SiC disk with abraded Kapton was irradiated with 80 mJ cm^{-2} at a repetition rate of 0.086 Hz. This is well below the frequency where accumulative heating from the laser is important.[48] The spectra match very well the spectra from the experiments using 10 Hz. The only difference is an enhanced absorption of the band at 2270 cm^{-1}, suggesting that in the experiments with higher repetition rates additional thermal decomposition of the isocyanate group takes place.

155 mJ cm^{-2}. At still higher fluences (155 mJ cm^{-2}) very pronounced changes in the IR spectra are detected even after one pulse (shown in Figure 9). Below 1100 cm^{-1} the background is rising extremely steeply, thus not allowing an analysis of bands in this region. This is, as discussed above, most probably due to carbonization of the irradiated surface, which leads to an overall increase of the IR absorption in this region.[38,46] This is supported by the black optical appearance of the SiC disk in the irradiated area. With increasing pulse numbers the shift of the baseline is even more pronounced; therefore, only the spectrum after one pulse can be analyzed. Similar features as for the lower fluence irradiations are observed. The bands of the imide system, aromatic ring, and the diaryl ether group are decreasing, while the bands connected with the amide and the isocyanate group are increasing. One observed difference is the absence of the increasing band at 1730 cm^{-1}. This band was assigned to stretching vibration of a carbonyl group attached to an aromatic system. In Figure 1b the SEM picture of a SiC disk after irradiation with 20 pulses at 155 mJ cm^{-2} is shown. The difference between the irradiated area and the unirradiated area is clearly visible (top right area is not irradiated). In the irradiated area the Kapton scrapes (see Figure 1a) are not observed any more, although the IR spectra still suggest the presence of Kapton.

Products of Laser Ablation. The volatile products of laser ablation of a Kapton film were measured with quadrupole mass spectrometer and with emission spectroscopy using the same Kapton samples and experimental setup as for the DRIFT measurements. In the mass spectra C_2H_2, HCN, CO, CO_2, C_4H_2, and C_6H_2 could be detected, while the emission spectra showed the C_2 and CN emission lines. The chemical species in the mass spectra were assigned according to refs 21 and 22, which used gas-phase FTIR and GC-MS for the assignment of the decomposition products.

Irradiation below the Threshold of Ablation: with 10 mJ cm^{-2}. A Kapton sample was irradiated at 1 Hz repetition rate (to exclude thermal effects) to test whether even below the threshold of ablation any signs of degradation can be observed. After 7500 pulses small changes in the spectrum are detected. Our mass spectrometry setup is not sensitive enough to detect this small amount of ablation products, but in studies using a quartz microbalance (e.g., ref 20) a reduction of the polymer mass at this low fluences was detected. Therefore, it can be assumed that (if at all) only portions of the ablation products are trapped within the polymer. The spectra match the previously described changes after irradiation with higher fluences and much lower pulse numbers.

Discussion

Laser irradiation with a fluence equal to the threshold fluence of ablation results in a slow decomposition of the polymer. The changes in the peak areas of several selected bands suggest a decomposition pathway as follows.

The bands corresponding to the imide system (1780, 1745, 1390, and 725 cm^{-1}) are decreasing. The changes in the peak area (shown in Figure 5 for the C═O band) are very similar for all of these bands. Corresponding to the decrease of these bands is an increase of the bands at 1730, 1500, and 1375 cm^{-1} (shown in Figure 5). These bands are assigned to species resulting from the breakage of the −N−(CO)− band in the imide system. The resulting structure is an amide system, with a C−N bond (1375 cm^{-1}), an aryl−C═O (1730 cm^{-1}), and an amide −(CO)−N− group (1780 cm^{-1}), shown in Figure 7. The band at 1260 cm^{-1}, assigned to the C_{ar}−O−C_{ar} group, decreases in a very similar manner (shown in Figure 5) to the bands assigned to the imide system. Corresponding to this decrease is an increase of a band at 1245 cm^{-1}, assigned to a C_{ar}−O stretching vibration. Therefore, we suggest in Figure 7 the following reaction pathway. The imide system breaks between the imide N and carbonyl carbon with a simultaneous decomposition of the diaryl ether group, either in the same repetition unit or at some other place along the polymer chain. Upon further laser irradiation a constant concentration of these species is maintained, suggesting that creation and decomposition of these groups reach a quasi-steady state.

This first step is probably photon-induced, but we cannot rule out that the temperature rise, which will take place during irradiation, is also important. A temperature rise can also increase the efficiency of photochemical reactions.[49] It would be very difficult to calculate a temperature rise, because the temperature rise is closely related to the absorption depth of the laser irradiation and depends on the lifetime and absorption of reaction intermediates. The lifetime is strongly dependent on the complexity of the molecules. The more complex the molecule, the longer the lifetime. In the condensed phase as in the case of PI, such intermediates can last for time periods of the order of nanoseconds (laser pulse ∼20 ns). The importance of this to the UV-laser decomposition of PI lies in the UV absorption characteristics of free-radical intermediates. Their strongly delocalized electrons will result in a more intense absorption of the incoming radiation than PI itself. However, their contribution to the absorption will be determined by their stationary concentration, i.e., their rate of formation less their rate of disappearance. We do not have these data; therefore, we cannot calculate the temperature rise.

In the next steps which could also be thermally induced, the aromatic systems (3080, 1600, and 1515 cm^{-1}) decompose, while acetylenes (3320 and 2255 cm^{-1}) are formed. At the same time isocyanate species are detected (2270 cm^{-1}), which decompose upon further irradiation or by reaction with other species (e.g., water to form amines). This decomposition is at least partially thermal, because at low repetition rates (0.086 Hz as compared to 10 Hz) the decrease of the isocyanate band is less pronounced. In the following steps nitrile (2230 cm^{-1}) and aliphatic hydrocarbons (CH) are formed (2950 cm^{-1}), as shown in Figure 8. The increase of the peak area of the aliphatic CH compounds is slower and nearly

linear with pulse numbers, suggesting that these species are formed continuously, probably through combination reactions. The volatile products detected by mass spectrometry and emission spectra are compatible with the mechanism described in Figure 7. The laser fluence or the corresponding temperature increase is most probably high enough to eliminate the CO group simultaneously from the amide system.

To clarify whether the overall decomposition reaction is purely thermal, additional experiments were performed. First we compared our data and reference mass spectra with mass spectra obtained during pyrolysis of Kapton.[50,51] The main products from pyrolysis are derived from a single benzene ring such as C_6H_5CN, C_6H_5OH, $C_6H_5NH_2$, $C_6H_4(CN)_2$, *p*-aminophenol, and C_6H_5NC. Benzene and its derivatives are only minor products during laser ablation. CN, also seen in the emission spectra, and HCN are important products of laser ablation, while they are not detected during pyrolysis. During pyrolysis neither small (C_1, C_2, or C_3) fragments nor carbon clusters ($>C_{38}$) are seen while they are abundant during UV-laser ablation. Then additional DRIFT experiments were performed: DRIFT spectra were recorded at different temperatures in an air stream. The spectra were analyzed analogous to the laser experiments. The difference spectra only showed a continuous decomposition of the complete polymer without pronounced intermediates. This is completely different from the laser experiments and clearly suggests that the laser photons and therefore the photochemical step play an important role. The temperature DRIFT experiments could be used to develop a decomposition model and to calculate even kinetic parameters of the polymer decomposition at localized sites (functional groups) in the polymers.

The SEM picture (Figure 1b) shows the SiC disk after irradiation with 20 pulses at 155 mJ cm^{-2}. The irradiated area is clearly visible (lower left area). No distinct polymer scrapes are visible, while the IR spectra still reveal the typical bands of Kapton. A possible explanation could be the degradation of the polymer to lower molecular weight species, which soften/flow to build a homogeneous layer on the SiC disk.

Upon irradiation with fluences below the threshold of ablation (10 mJ cm^{-2}) changes in the DRIFT spectra are observed. These in principle unexpected changes could be due either to imperfections in the laser beam profile, resulting in partial higher fluences, or to a slow photolytic decomposition of Kapton not resulting in ablation of the polymer. The latter could also account for the difference in the threshold fluences measured by mass sensitive techniques (QMB) and surface morphology sensitive techniques (AFM). Gaseous decomposition products, such as CO, CO_2, HCN, and C_2H_2, could be ejected without changing the surface morphology. This would be detected by QMB, which indeed suggests a lower ablation threshold than AFM.

Conclusion

Silicon carbide (SiC) is a suitable substrate for studies of laser-induced process in polymers. The SiC substrate is stable under the applied conditions, i.e., fluences up to 155 mJ cm^{-2}, and well-resolved DRIFT spectra of polymers can be obtained. The surface sensitive DRIFT technique allows a detection of reaction intermediates and products of the laser-treated *solid* polymer. The first step of the UV-laser (308 nm)-induced decomposition of the polyimide (Kapton) is the simultaneous breakage of the nitrogen−(carbonyl carbon) bond of the imide system and of the diaryl ether group. The resulting species belonging to the amide system and aromatic carbonyl groups are detected. Decomposition of the aromatic system is detected also, and an isocyanate-rich surface is formed. In the next steps aliphatic hydrocarbons, nitriles, and alkynes are created. Volatile species compatible with this decomposition mechanism (CO, CO_2, HCN, and C_2H_2) are identified by mass spectrometry. Even below the threshold of ablation a decomposition of the polymer is detected. This could be due to either inhomogeneities in the beam profile or real decomposition of the polymer at this fluence. The latter could also explain the differences in the threshold fluence measured with QMB and AFM. The QMB would detect the removal of gaseous species which could happen without structuring of the polymer.

Acknowledgment. Financial support of the Swiss National Science Foundation is gratefully acknowledged. The authors are also grateful to Dr. J. Wambach and Dr. M. Meli for fruitful discussions.

References and Notes

(1) Sroog, C. E. In *Polyimides-Fundamental and Applications*; Gosh, M. K., Mittal, K. L., Eds.; Marcel Dekker: New York, 1996; p 1.
(2) Dimitrakopoulos, C. D.; Machlin, E. S.; Kowalczyk, S. P. *Macromolecules* **1996**, *29*, 5818.
(3) Matsumoto, T. *Macromolecules* **1999**, *32*, 4933.
(4) Hasegawa, M.; Sensui, N.; Shindo, Y.; Yokota, R. *Macromolecules* **1999**, *32*, 387.
(5) Chern, Y. T. *Macromolecules* **1998**, *31*, 5837.
(6) Pyo, S. M.; Kim, S. I.; Shin, T. J.; Park, H. K.; Ree, M.; Park, K. H.; Kang, J. S. *Macromolecules* **1998**, *31*, 4777.
(7) Chen, J. P.; Labarthet, F. L.; Natansohn, A.; Rochon, P. *Macromolecules* **1999**, *32*, 8579.
(8) Wilson, A. In *Polyimides*; Mittal, K. L., Ed.; Plenum: New York, 1984; p 715.
(9) Kawakami, H.; Mikawa, M.; Nagaoka, S. *Macromolecules* **1998**, *31*, 6636.
(10) Coleman, M. R.; Koros, W. J. *Macromolecules* **1999**, *32*, 3106.
(11) Andrew, E.; Dyer, P. E.; Forster, D.; Key, P. E. *Appl. Phys. Lett.* **1983**, *43*, 717.
(12) Srinivasan, R.; Braren, B. *J. Polym. Sci.* **1984**, *22*, 2601.
(13) Pettit, G. H. In *Polyimides-Fundamental and Applications*; Gosh, M. K., Mittal, K. L., Eds.; Marcel Dekker: New York, 1996; p 453.
(14) Bachman, F. *Chemtronics* **1989**, *4*, 149.
(15) Lankard, J. R.; Wolbold, G. *Appl. Phys. A* **1992**, *54*, 355.
(16) E.g.: Aoki, H. US Patent 5736999, issued 04/1998.
(17) Hansen, S. G.; Robitaille, T. E. *Appl. Phys. Lett.* **1988**, *52*, 81.
(18) Brannon, H.; Lankard, J. R.; Baise, A. I.; Burns, F.; Kaufman, J. *J. Appl. Phys.* **1985**, *58*, 2036.
(19) Küper, S.; Brannon, J.; Brannon, K. *Appl. Phys. A* **1993**, *56*, 43.
(20) Arnold, N.; Bityurin, N. *Appl. Phys. A* **1999**, *68*, 615.
(21) Srinivasan, R.; Hall, R. R.; Wilson, W. D.; Loehle, W. D.; Allbee, D. C. *J. Appl. Phys.* **1995**, *78*, 4881.
(22) Singleton, D. L.; Paraskevopoulos, G.; Irwin, R. S. *J. Appl. Phys.* **1989**, *66*, 3324.
(23) Ulmer, G.; Hasselberger, B.; Busman, H.-G.; Campbell, E. E. B. *Appl. Surf. Sci.* **1990**, *46*, 272.
(24) Koren, J.; Yeh, J. T. C. *J. Appl. Phys.* **1984**, *56*, 2120.
(25) Srinivasan, R.; Braren, B.; Dreyfus, R. *J. Appl. Phys.* **1987**, *61*, 372.
(26) Feurer, T.; Sauerbrey, R.; Smayling, M. C.; Story, B. J. *Appl. Phys. A* **1993**, *56*, 275.
(27) Ball, Z.; Sauerbrey, R. *Appl. Phys. Lett.* **1994**, *65*, 391.
(28) Lippert, T.; Ortelli, E.; Panitz, J.-C.; Raimondi, F.; Wambach, J.; Wei, J.; Wokaun, A. *Appl. Phys. A* **1999**, *69*, S651.
(29) Moyses, S.; Spells, S. J. *Macromolecules* **1999**, *32*, 2684.
(30) Shimomura, M.; Okumoto, H.; Kaito, A.; Ueno, K.; Shen, J. S.; Ito, K. *Macromolecules* **1998**, *31*, 7843.

(31) Minagawa, M.; Yoshida, W.; Kurita, S.; Takada, S.; Yoshii, F. *Macromolecules* **1997**, *30*, 1782.
(32) Snively, C. M.; Koenig, J. L. *Macromolecules* **1998**, *31*, 3753.
(33) Buback, M.; Kowollik, C. *Macromolecules* **1998**, *31*, 3211.
(34) Ozaki, Y.; Liu, Y. L.; Noda, I. *Macromolecules* **1997**, *30*, 2391.
(35) Ren, Y. Z.; Murakami, T.; Nishioka, T.; Nakashima, K.; Noda, I.; Ozaki, Y. *Macromolecules* **1999**, *32*, 6307.
(36) Storey, R. F.; Donnalley, A. B. *Macromolecules* **1999**, *32*, 7003.
(37) Kokai, F.; Saito, H.; Fujioka, T. *Macromolecules* **1990**, *23*, 674.
(38) Mihailov, S.; Duley, W. *SPIE−Laser Beam Surface Treating and Coating* **1988**, *957*, 111.
(39) Yeboah, S. A.; Wang, S.-H.; Griffiths, P. R. *Appl. Spectrosc.* **1984**, *38* (2), 259.
(40) Si-Carb sampler using 320-grid-Carb paper obtained from Spectra-Tech. This sampling kit for diffuse reflectance cells allows the analysis of intractable samples such as hard polymers, paints, and coatings. A small disk of silicon carbide paper is used to abrade the sample surface to transfer a small amount of material to the DRIFT cell.
(41) Kubelka, P.; Munk, F. *Z. Tech. Phys.* **1931**, *11*, 593.
(42) Ehlers, G. F. L.; Fisch, K. R.; Powell, W. R. *J. Polym. Sci.* **1970**, *8*, 3511.
(43) Ishida, H.; Wellinghoff, S. T.; Baer, E.; Koenig, J. L. *Macromolecules* **1980**, *13*, 826.
(44) Brekner, M. J.; Geger, C. *J. Polym. Sci.* **1987**, *25A*, 2005.
(45) Socrates, G. *Infrared Characteristic Group Frequencies*; J. Wiley & Sons: New York, 1994.
(46) Borisevich, N. A.; Khovratovich, N. N. *Opt. Spectrosc.* **1961**, *10*, 309.
(47) Molis, S. In *Proceedings of Third International Conference on Polyimides* **1988**, 87.
(48) Ball, Z.; Feurer, T.; Callahan, D. L.; Sauerbrey, R. *Appl. Phys. A* **1996**, *62* 203.
(49) Graham, J. L.; Berham, J. M.; Dellinger, B. *J. Photochem. Photobiol. A* **1993**, *71*, 65.
(50) Sroog, C. E. *Polym. Sci. Macromol. Rev.* **1976**, *11*, 176.
(51) Dussel, J.-J.; Rosen, H.; Hummel, D. O. *Makromol. Chem.* **1976**, *177*, 2343.

MA000389A